Title
Arg-Gly-Asp-D-Phe-Lys peptide-modified PEGylated dendrimer-entrapped gold nanoparticles for targeted computed tomography imaging of breast carcinoma.

Journal
Nanomedicine (London, England), 10(14)

ISSN
1743-5889

Authors
Li, Kangan
Zhang, Zhuoli
Zheng, Linfeng
et al.

Publication Date
2015-07-01

DOI
10.2217/nnm.15.59

Peer reviewed

Research Article

For reprint orders, please contact: reprints@futuremedicine.com

Nanomedicine

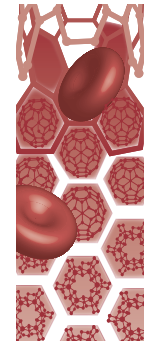

Arg-Gly-Asp-D-Phe-Lys peptide-modified PEGylated dendrimer-entrapped gold nanoparticles for targeted computed tomography imaging of breast carcinoma

Aim: To investigate cyclo (Arg-Gly-Asp-D-Phe-Lys) peptide (RGD)-modified PEGylated dendrimer-entrapped gold nanoparticles (PEGylated Au DENPs-RGD) for targeted computed tomography (CT) imaging of breast carcinomas. **Materials & methods:** PEGylated Au DENPs-RGD were synthesized and characterized. Then, the PEGylated Au DENPs-RGD for targeted CT imaging were investigated using the MDA-MB-435 cell line, an integrin-rich breast carcinoma cells, and mice with MDA-MB-435 xenograft tumors. Finally, silver enhancement staining and integrin $\alpha_v\beta_3$ immunohistochemistry of the tumors were performed. **Results:** The synthesized PEGylated Au DENPs-RGD were spherical, water dispersible and biocompatible nanoprobes with a gold nanoparticle core size of 2.8 nm. Due to the presence of the Au nanoparticles, the PEGylated Au DENPs-RGD displayed a higher x-ray attenuation intensity than Omnipaque at the same Au or I concentrations. The conjugated RGD ligand can specifically identify and target overexpressed integrin receptors on MDA-MB-435 cells. After intravenous injection, these nanoprobes accumulated in the targeted area of mice with MDA-MB-435 xenograft tumors, which enabled the tumor to be detected by CT imaging. The histological results confirmed the imaging results. **Conclusion:** The PEGylated Au DENPs-RGD can be used as targeted nanoprobes with good biocompatibility for targeted CT imaging and diagnosis of integrin-positive tumors.

Keywords: breast carcinoma • dendrimers • gold nanoparticles • integrin • RGD peptides • targeted computed tomography imaging

Kangan Li*,‡,1, Zhuoli Zhang‡,2, Linfeng Zheng**,‡,1,2, Hong Liu4, Wei Wei3, Zhiyu Li1, Zhiyan He1, Andrew C Larson2 & Guixiang Zhang***,1

[1]Department of Radiology, Shanghai First People's Hospital, Shanghai Jiao Tong University, Shanghai 200080, China
[2]Department of Radiology, Feinberg School of Medicine, Northwestern University, Chicago, IL 60611, USA
[3]Department of General Surgery, Xiangya Hospital, Xiangya School of Medicine, Central South University, Changsha 410008, China
[4]Department of Gastroenterology and Hepatology, Shanghai First People's Hospital, Shanghai Jiao Tong, University, Shanghai 200080, China
*Author for correspondence:
Tel.: +86 21 63240090/4170
Fax: +86 21 63240825
kangan.li@sjtu.edu.cn
**Author for correspondence:
Tel.: +86 21 63240090/4173
Fax: +86 21 63240825
zhenglinfeng04@aliyun.com
***Author for correspondence:
Tel.: +86 21 63240090/4166
Fax: +86 21 63240825
guixiangzhang@sina.com
‡Authors contributed equally

Recently, the development of molecular imaging has provided a significant amount of information for the early and accurate diagnosis of cancer via different imaging modalities [1,2]. Computed tomography (CT) imaging is one of the most popular imaging modality in the clinical field because of its low cost, wide availability and efficiency [3–8]. It provides high spatial resolution and can obtain functional information about tissues through the use of contrast materials [9]. In addition to imaging modalities, nanoparticle probes with high specificity and sensitivity play crucial roles in molecular imaging. Appropriate biomedical probes are typically achieved via the conjugation of targeting ligands for improved affinity and targeting efficiency [10,11].

The Arg-Gly-Asp (RGD) peptide is an effective ligand for tumor targeting because it can specifically bind with integrin $\alpha_v\beta_3$, a cell adhesion molecule that plays a significant role in regulating tumor growth, angiogenesis and metastasis [12,13]. Integrin $\alpha_v\beta_3$ is overexpressed not only in many cancer cell lines but also in tumor endothelium tissue [14,15]. Some published studies have used ligands to bind receptors that are primarily overexpressed on cancer cells, such as folate or transferrin receptor [16,17]. Therefore, nanoparticle probes grafted with the RGD peptide may be considered a superior targeting system. The high affinity interaction between the RGD peptides and the cancer-related integrins has led to the widespread use of RGD peptide sequences as ligands for integrin-targeted applications [18].

Future Medicine part of fsg

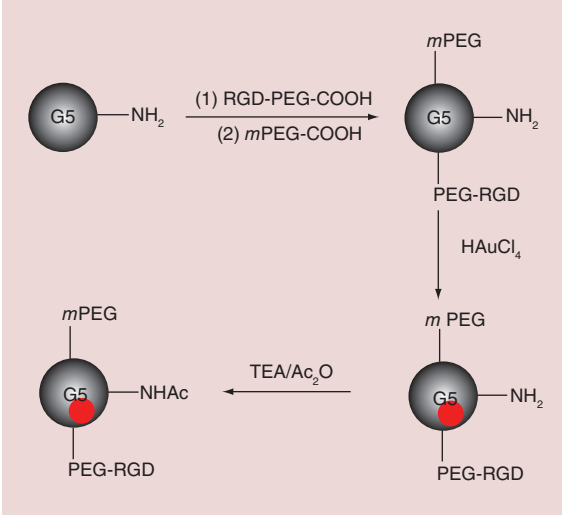

Figure 1. Schematic illustration of the preparation of the {$(Au^0)_{300}$-G5.NHAc-$(PEG\text{-}RGD)_7$-*m*PEG_8} dendrimer-entrapped nanoparticles.
RGD: Arg-Gly-Asp-D-Phe-Lys.

Colloidal gold nanoparticles (Au NPs) are an attractive candidate for use as x-ray CT imaging probes because they offer several advantages over traditional iodine-based agents. First, Au NPs exhibit little or no cytotoxicity within a certain concentration range [16,19–21]. Second, gold has a higher attenuation intensity than iodine and, consequently, a higher CT contrast ability. Additionally, Au NPs can be easily modified with biomolecules via thiol-Au bonds and many other functional ligands can simultaneously be incorporated. Furthermore, some antibiofouling polymers, such as PEG, can be easily attached to Au NP surfaces to prepare highly stable and specific probes and permit the efficient conjugation of targeting ligands [5,22]. These attached polymers may also prolong the blood circulation time of the Au NPs by effectively decreasing the uptake and clearance by the reticuloendothelial system, which is particularly beneficial for targeted tumor imaging with ligand-modified nanocarriers [5,22,23].

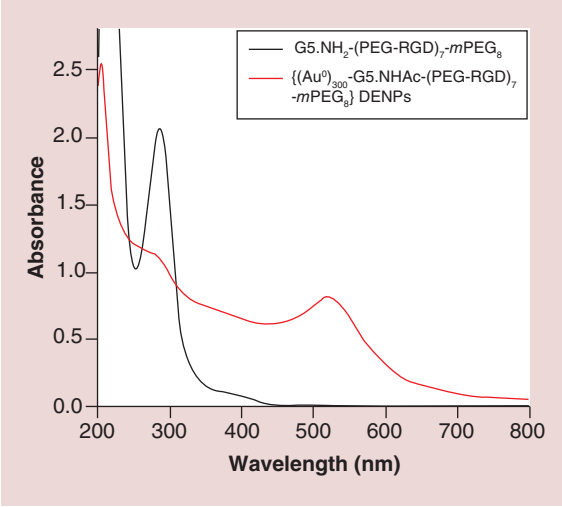

Figure 2. UV-vis spectra of G5.NH_2-$(PEG\text{-}RGD)_7$-*m*PEG_8 and {$(Au^0)_{300}$-G5.NHAc-$(PEG\text{-}RGD)_7$-*m*PEG_8} DENPs dispersed in water (pH = 6.0) at room temperature (25°C).
DENP: Dendrimer-entrapped nanoparticle; RGD: Arg-Gly-Asp-D-Phe-Lys.

Among the many polymer-based approaches for synthesizing NP-based contrast agents, dendrimers, which are highly branched synthetic macromolecules with an internal cavity and massive groups on the surface [24], have been utilized as versatile templates to synthesize various inorganic NPs [4,5,16,20,25–31] or to modify their surfaces [7] for CT imaging applications. In addition, the unique structural properties of dendrimers, including highly branched, monodispersed and synthetic macromolecules allow them to be used as an ideal platform to form NPs for the diagnosis and therapeutic treatment of cancer [32–35].

In our previous work [4,5,30], we described the synthesis and characterization of dendrimer-entrapped gold nanoparticles (Au DENPs) modified with PEG with enhanced biocompatibility for CT imaging applications. In the present study, G5.NH2 dendrimers are premodified with methoxyl polyethylene glycol acid (*m*PEG-COOH) and the targeting ligand (cyclic RGD) via a PEG linker strategy. Then, the G5.NH_2-$(PEG\text{-}RGD)_7$-*m*PEG_8 products were used as templates to entrap Au NPs. Following acetylation of the remaining dendrimer terminal amines, integrin-targeted {$(Au^0)_{300}$-G5.NHAc-$(PEG\text{-}RGD)_7$-*m*PEG_8} DENPs (PEGylated Au DENP-RGD) were obtained (Figure 1). The PEGylated Au DENP-RGD probes were characterized via UV-vis spectrometry, inductively coupled plasma-atomic emission spectroscopy (ICP-AES) and transmission electron microscopy (TEM). Cytotoxicity assays were used to assess the cytocompatibility of the particles. Targeted CT imaging performance was evaluated *in vitro* and *in vivo* using a breast carcinoma cell line (MDA-MB-435) and a xenografted tumor model, respectively. Histological studies of the *in vivo* tumor uptake of the PEGylated Au DENP-RGD probes and expression of integrin $\alpha_v\beta_3$ on MDA-MB-435 xenograft tumors confirmed targeting of tumor by the NPs. *In vivo* studies of biodistribution show that the NPs can be cleared in 96 h. To the best of our knowledge, this is the first report describing the development of integrin-targeted PEGylated Au DENPs-RGD as a probe for the targeted CT imaging of tumors.

Materials & methods

Materials

Methoxyl polyethylene glycol acid was purchased from Nanocs, Inc. (NY, USA). The cyclo (Arg-Gly-Asp-D-

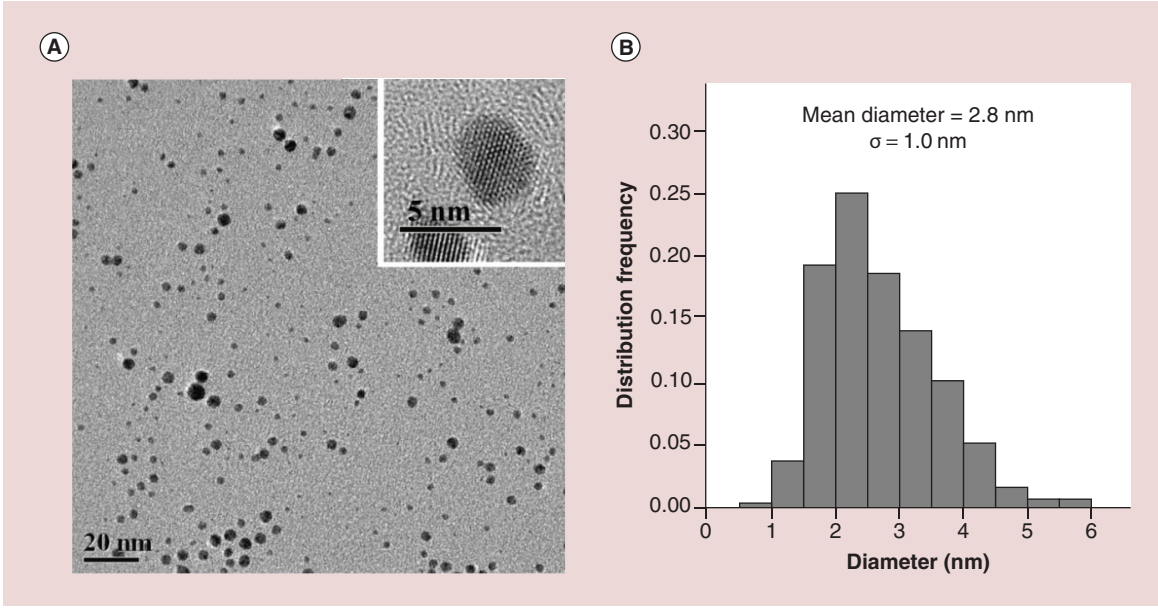

Figure 3. Transmission electron microscope image and size distribution histogram of the PEGylated Au DENPs-RGD. (A) Transmission electron microscope image. **(B)** Size distribution histogram. The insert of **(A)** shows selected high-resolution area.
PEGylated Au DENPs-RGD: PEGylated dendrimer-entrapped gold nanoparticles-Arg-Gly-Asp-D-Phe-Lys.

Phe-Lys) peptide [c(RGDyk)] and the cyclo (Arg-Gly-Asp-D-Phe-Lys)-polyethylene glycol-COOH (RGD-PEG-COOH) peptide were purchased from Peptides International, Inc. (KY, USA). Anti-integrin $\alpha_v\beta_3$ antibody, clone LM609 and integrin $\alpha_v\beta_3$ inhibitor Cilengitide (EMD 121974) were obtained from Merck Millipore (Merck KGaA, Darmstadt, Germany). Ethylenediamine amine-terminated poly amidoamine dendrimers of generation 5 ($G5.NH_2$) with a polydispersity index less than 1.08 were purchased from Dendritech (MI, USA). All other chemicals were purchased from Sigma-Aldrich (Shanghai, China). The MDA-MB-435 cell line was obtained from the Shanghai Cell Bank (Shanghai, China). Regenerated cellulose dialysis membranes were purchased from Fisher (PA, USA). Water purified with a Milli-Q Plus 185 water purification system (Millipore, MA, USA) was used in all of the experiments.

Synthesis & characterization of targeted PEGylated Au DENPs-RGD

Ten molar equivalents of RGD-PEG-COOH (0.015 mmol, 46.32 mg) were dissolved in dimethyl sulphoxide (DMSO), activated by reacting with EDC/NHS for approximately 3 h, and then added to a solution of $G5.NH_2$ dendrimers (1.54×10^{-3} mmol, 40.16 mg) in DMSO (10 ml) dropwise under vigorous magnetic stirring. The stirring process required 3 days to finish the reaction. Then, ten molar equivalents of *m*PEG-COOH (0.031 mmol, 30.88 mg) were dissolved in DMSO, activated by reacting with EDC/NHS for approximately 3 h, and then added to a solution of RGD-PEG-modified $G5.NH_2$ dendrimers (1.54×10^{-3} mmol, 40.16 mg) in DMSO (10 ml) dropwise under vigorous magnetic stirring. To complete the reaction, the stirring process required another 3 days. During this time, the reaction mixture slowly turned faint yellow. The reaction mixture was then dialyzed against phosphate-buffered saline (PBS) buffer (4 liters, three-times) and water (4 liters, three-times) to remove excess reactants and by-products for 3 days. The $G5.NH_2$-$(PEG\text{-}RGD)_7$-*m*PEG_8 product was obtained by lyophilization.

The procedures used to synthesize the $\{(Au^0)_{300}$-$G5.NH_2$-$(PEG\text{-}RGD)_7$-*m*$PEG_8\}$ DENPs were based on previously reported methods [25,26,36]. The $\{(Au^0)_{300}$-$G5.NH_2$-$(PEG\text{-}RGD)_7$-*m*$PEG_8\}$ DENPs were prepared using sodium borohydride reduction chemistry with a $G5.NH_2$ to gold salt molar ratio of 300:1. Briefly, the $HAuCl_4$ solution was added to an aqueous solution of G5.NH2-$(PEG\text{-}RGD)_7$-*m*PEG_8 (the molar ratio of $G5.NH_2$ to the gold salt is 300:1) under vigorous stirring. After 30 min, a 5-fold molar excess of ice-cold $NaBH_4$ solution was added to the dendrimer/gold salt mixture with stirring. The reaction mixture turned deep red within a few seconds. Completing the reaction required 2 h of continuous stirring. The final products are denoted $\{(Au^0)_{300}$-$G5.NH_2$-$(PEG\text{-}RGD)_7$-*m*$PEG_8\}$ DENPs. Then, the remaining dendrimer terminal amine groups of the $\{(Au^0)_{300}$-$G5.NH_2$-$(PEG\text{-}RGD)_7$-*m*$PEG_8\}$ DENPs were acetylated [25,37–38]. Briefly, with continuous magnetic stirring, triethylamine (at a fourfold molar excess over the

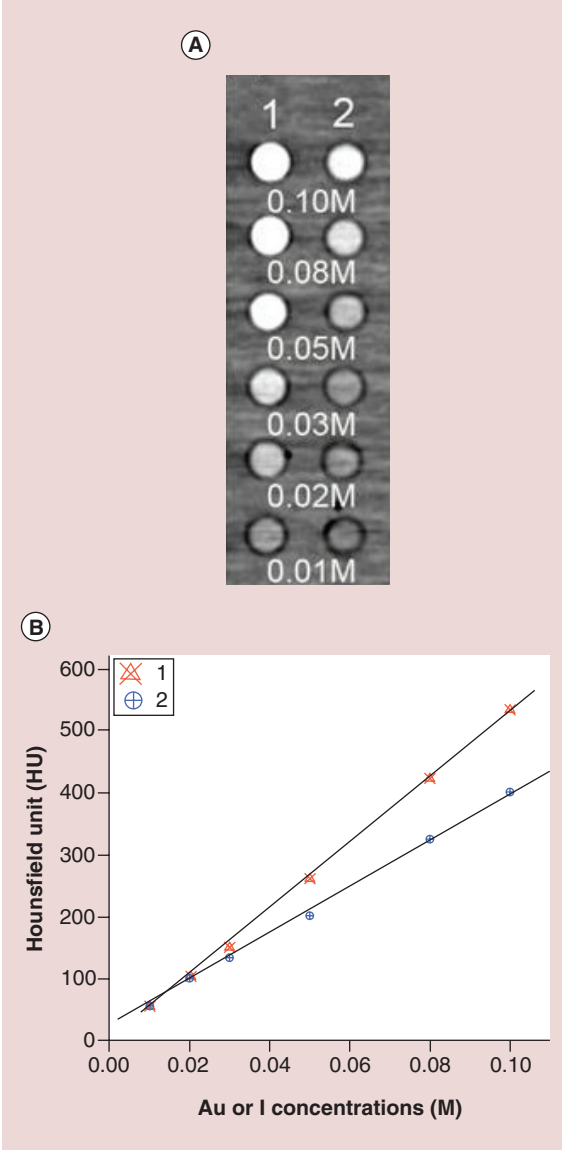

Figure 4. Computed tomography image and x-ray attenuation (HU) of PEGylated Au DENPs-RGD (1) and Omnipaque (2) as a function of the molar concentration of the radiodense element (Au or iodine). **(A)** Computed tomography image. **(B)** X-ray attenuation.
PEGylated Au DENPs-RGD: PEGylated dendrimer-entrapped gold nanoparticles-Arg-Gly-Asp-D-Phe-Lys.

total primary amines of G5.NH_2) was added to an aqueous solution of {$(Au^0)_{300}$-G5.NH_2-$(PEG\text{-}RGD)_7$-*m*PEG_8} DENPs. Thirty min later, acetic anhydride (at the same molar ratio as triethylamine) was added to the triethylamine/DENP mixture under continuous stirring, and the mixture was reacted for 24 h. Finally, the aqueous solution of the reaction mixture was dialyzed against PBS buffer (4 liters, three-times) and water (4 liters, three-times) to remove excess reactants and by-products for 3 days, then the targeted {$(Au^0)_{300}$-G5.NHAc-$(PEG\text{-}RGD)_7$-*m*PEG_8} DENPs (PEGylated Au DENPs-RGD) were obtained by lyophilizing. Nontargeted PEGylated Au DENPs were prepared according to previously reported methods [5].

TEM was performed using a JEOL 2010F analytical electron microscope (JEOL Ltd, Tokyo, Japan). The diluted suspension of PEGylated Au DENPs-RGD (1 mg/ml, 5 µl) were deposited on to a carbon-coated copper grid and then air-dried prior to performing the measurements. After capturing digital images, 300 NPs of each sample were randomly selected to measure the size using ImageJ software [39] and the size distribution histogram of the PEGylated Au DENPs-RGD was drawn. UV-vis spectra were collected using a Lambda 25 UV-vis spectrometer (PerkinElmer, MA, USA). PEGylated Au DENPs-RGD samples were dissolved in water before analysis. ICP-AES (Teledyne Leeman Labs, NH, USA) was used to analyze the amount of Au in the PEGylated Au DENPs-RGD. CT scans were performed using a 64-row detector system (Discovery CT750 HD, GE Healthcare, WI, USA) at 80 kV and 100 mA. Then, 0.2 ml of solutions with different Au concentrations of PEGylated Au DENPs-RGD in 1.5 ml Eppendorf tubes were scanned. The CT values of each sample were calculated in Hounsfield units (HU).

Cell culture

MDA-MB-435 cells were continuously cultured in a 37°C incubator with 5% CO_2 in RPMI-1640 medium supplemented with 10% heat-inactivated foetal bovine serum, 100 U/ml penicillin and 100 µg/ml streptomycin.

The NK-92MI cell line was purchased from the American Type Culture Collection (ATCC, VA, USA) and grown according to the ATCC recommended culturing procedure.

In vitro cytotoxicity assay

The cytotoxicity of the PEGylated Au DENPs-RGD was first evaluated using a 3-(4,5-dimethylthiazol-2-yl)-2,5-diphenyltetrazolium bromide (MTT) colorimetric assay. Briefly, 1×10^4 MDA-MB-435 or NK-92MI cells/well were seeded in 96-well cell culture plates with complete medium. After culturing overnight to bring the cells to approximately 80% confluence, the medium was replaced with complete medium containing PEGylated Au DENPs-RGD with a final Au concentration ranging from 0 to 100 µM. After 24 h of incubation at 37°C and with 5% CO_2, MTT (10 µl, 5 mg/ml) in PBS was added and the incubation was continued for another 4 h. The medium in the plates was then removed, and 200 µl of DMSO was added. The absorbance values at a wavelength of 570 nm in each well were measured using a Thermo MK3 ELISA reader (USA). The means and standard devia-

tions of the wells were recorded based on three measurements. Meanwhile, MDA-MB-435 cells were observed after treatment with the PEGylated Au DENPs-RGD for 24 h using an Olympus BX53microscope (Tokyo, Japan) at a magnification of 200× .

In vitro cellular uptake assay

The cellular uptake of PEGylated Au DENPs-RGD by target cells was evaluated using ICP-AES. Briefly, MDA-MB-435 cells were seeded separately into 24-well plates. After culturing overnight to bring the cells to confluence, the medium was replaced with fresh medium containing PEGylated Au DENPs-RGD ([Au] = 0, 20 and 40 μM, n = 6) and 100 μl of integrin $\alpha_v\beta_3$ inhibitor (Cilengitide, EMD 121974), 2 h before the addition of PEGylated Au DENPs-RGD ([Au] = 0, 20 and 40 μM, n = 6) and nontargeted PEGylated Au DENPs ([Au] = 0, 20 and 40 μM, n = 6). The cells were then incubated for 4 h, washed three-times with PBS buffer, trypsinized and resuspended with PBS buffer. After counting the cell number, the cell pellets were acquired using centrifugation and then digested using 0.5 ml of aqua regia solution. Then, Au uptake by the cells was quantified using ICP-AES.

In vitro targeted CT imaging of cancer cells

To explore the potential for targeted CT imaging of cancer cells *in vitro* with PEGylated Au DENPs-RGD probes, MDA-MB-435 cells were divided into three groups. Approximately 5 × 10^6 MDA-MB-435 cells were plated into each 5 ml cell culture flask overnight to bring the cells to approximately 80% confluence. Then, the medium in the first group was replaced with 5 ml of medium containing PEGylated Au DENPs-RGD ([Au] = 0, 10, 20, 40, 80 and 100 μM). The medium in the second group was replaced with fresh medium containing 100 μl of the RGD-peptide inhibitor of integrin $\alpha_v\beta_3$ (Cilengitide, EMD 121974), 2 h before the addition of PEGylated Au DENPs-RGD ([Au] = 0, 10, 20, 40, 80 and 100 μM). Finally, the medium in the third group was replaced with fresh medium containing nontargeted PEGylated Au DENPs ([Au] = 0, 10, 20, 40, 80 and 100 μM). After incubating for 4 h, the cells were transferred to 1.5 ml Eppendorf tubes. Then, the tubes with cell suspension were scanned using a 64-row detector system (Discovery CT750 HD, GE healthcare) at 80 kV and 100 mA. The CT values were acquired on a workstation supplied by the manufacturer. Each experiment was conducted in triplicate.

In vivo targeted CT imaging of a xenograft tumor model

Animal experiments were performed according to protocols approved by the institutional committee for animal care of the Shanghai First People's Hospital. Twenty four female 4–6 week old BALB/c nude mice (SLAC Laboratory Animal Center, Shanghai) were subcutaneously injected with 1 × 10^6 MDA-MB-435 cells/mouse in the right oxter. Approximately 3 weeks postinjection, when the tumor nodules reached a volume of 0.5–1 cm^3, the mice were anesthetized with an intraperitoneal injection of pentobarbital sodium (40 mg/kg) and were then randomly divided into three groups: one group received 200 μl of the PEGylated Au DENPs-RGD ([Au] = 0.1 M) via the tail vein (n = 8), the second group received 200 μl of the integrin $\alpha_v\beta_3$ inhibitor (Cilengitide, EMD 121974) intraperitoneally 2 h before delivering 200 μl of PEGylated Au DENPs-RGD ([Au] = 0.1 M) via the tail vein (n = 8) [40], and the last group received nontargeted PEGylated Au DENPs ([Au] = 0.1 M) at a similar dose (n = 8). The CT scans were performed

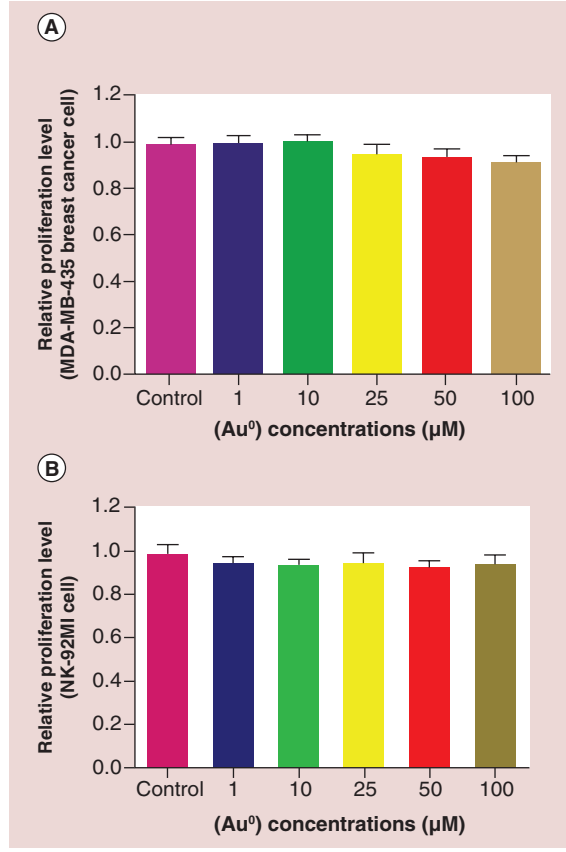

Figure 5. MTT assay of the viability of MDA-MB-435 breast carcinoma cells (A) and NK-92MI human natural killer cells (B) treated with PEGylated Au DENPs-RGD at different Au concentrations for 24 h. For both MDA-MB-435 breast carcinoma cells and NK-92MI cells, there was no statistical significance between the PBS control and the cells treated with different Au concentrations (all $p > 0.05$, n = 3).
PEGylated Au DENPs-RGD: PEGylated dendrimer-entrapped gold nanoparticles-Arg-Gly-Asp-D-Phe-Lys.

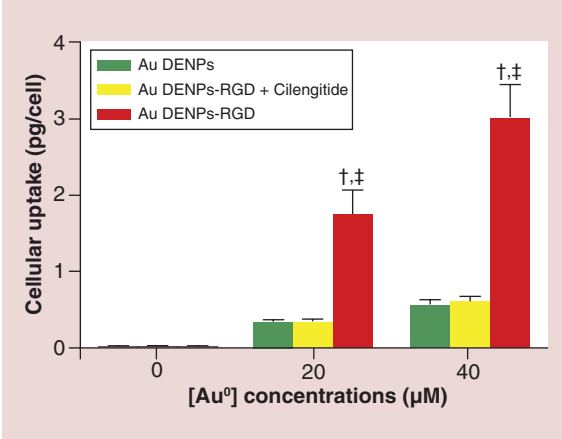

Figure 6. Cellular uptake of Au in MDA-MB-435 breast cancer cells treated with targeted PEGylated Au DENPs-RGD, nontargeted PEGylated Au DENPs, and targeted nanoparticles blocked by Cilengitide (a type of integrin $\alpha_v\beta_3$ inhibitor) with different Au concentrations for 4 h. The Au uptake in MDA-MB-435 cells treated with targeted PEGylated Au DENPs-RGD probes is significantly higher than in cells treated with nontargeted PEGylated Au DENPs probes (†$p < 0.01$; $n = 6$) and in blocked integrin $\alpha_v\beta_3$ cells that were treated with the same targeted nanoparticles (‡$p < 0.01$; $n = 6$).
PEGylated Au DENPs-RGD: PEGylated dendrimer-entrapped gold nanoparticles-Arg-Gly-Asp-D-Phe-Lys.

before and 2, 6 and 24 h postinjection of the particles using a micro-CT imaging system (SkyScan, Bruker, Belgium) with 80 kV, 450 μA and a slice thickness of 45 μm. Images were reconstructed and CT values were acquired on a micro-CT imaging workstation supplied by the manufacture.

Silver enhancement staining & integrin $\alpha_v\beta_3$ immunohistochemistry

Tumors resected from mice treated with different methods were washed twice with sterile PBS and embedded in paraffin for histological analysis. Silver enhancement staining was performed using a silver enhancement kit (Fitzgerald, MA, USA). Integrin $\alpha_v\beta_3$ immunohistochemistry was performed according to the manufacturer's instructions. Briefly, the tissues were incubated with rabbit antimurine monoclonal antibodies overnight at 4°C followed by incubating with rabbit polyclonal secondary antibodies for 2 h at room temperature. Tissue sections were washed three-times in PBS and then visualized with 3,3'-diaminobenzidine (DAB) for immunohistochemical analysis. The histological analysis of paraffin sections stained with hematoxylin and eosin was conducted as previously described [16,20]. Tissue sections were photographed with an Olympus BX53 compound microscope at a magnification of 200×.

In vivo distribution study

Six female BALB/c nude mice (22–25 g) bearing tumors were used for *in vivo* biodistribution studies of PEGylated Au DENPs-RGD. After anesthetization via intraperitoneal injection of pentobarbital sodium (40 mg/kg), the mice were intravenously injected with PEGylated Au DENPs-RGD (200 μl in PBS solution, [Au] = 0.1 M) via the tail vein at different time points (6, 24 and 96 h postinjection). Then, the mice were euthanized and the organs (including the heart, liver, spleen, lungs and kidneys) and tumors were extracted and weighed. The organs and tumors were digested in an aqua regia solution overnight. The Au uptake by the different organs and tumors was determined using ICP-AES.

Statistical analysis

One-way ANOVA statistical analysis was performed to evaluate the significance of the experimental data, and p-values less than 0.05 were considered significant.

Results & discussion

Synthesis & characterization of targeted PEGylated Au DENPs-RGD

The work reported here differs from our previous study related to the synthesis of Gd(III)-loaded Au DENPs (Gd-Au DENPs) [21], where only one type of PEG moiety (*m*PEG-COOH) was modified onto the G5 dendrimer surface for templated Au NP synthesis. In this study, mixed PEG moieties containing PEG segments (RGD-PEG-COOH and *m*PEG-COOH) with the same Mw, were sequentially conjugated to the G5.NH_2 surface via EDC coupling chemistry (Figure 1). The RGD peptides that are attached to the dendrimer surface are expected to enable the particles to specifically target cancer cells that overexpress integrin via ligand–receptor interactions. This approach is similar to our previous study [5] in which PEGylation of dendrimers not only allowed for a higher loading of Au compared with acetylated Au DENPs [25] but also significantly improved the stability of the targeted particles. The surface charge of PEGylated Au DENPs-RGD is neutral after acetylation, which has been previously reported by our group [41], and this property is important to avoid toxicity and nonspecific binding.

The optical properties of the PEGylated Au DENPs-RGD were characterized using UV-vis spectroscopy (Figure 2). The intermediate G5.NH2-$(PEG\text{-}RGD)_7$-$m(PEG)_8$ dendrimer product without entrapped Au NPs displays only the typical absorption peak of RGD at 280 nm. By contrast, the PEGylated Au DENPs-RGD particles have two characteristic absorption peaks: one at 520 nm, which is attributed to the typical surface plasmon resonance band of Au NPs, and one at

280 nm, which dramatically decreased after the addition of the Au NPs due to the overlap of RGD and Au NPs; this latter peak can be assigned to the conjugated RGD moieties for targeted imaging.

TEM was used to characterize the size and morphology of the PEGylated Au DENPs-RGD (Figure 3). The NPs are nearly spherical, and the mean size of the NPs is 2.8 ± 1.0 nm (Figure 3A & B). The crystalline nature of the targeted PEGylated Au DENPs-RGD was confirmed using high-resolution TEM imaging, where the lattice structure of the particles can be clearly observed (insert of Figure 3A). In our previous report, the hydrodynamic size of Gd-Au DENP-RGD NPs measured using dynamic light scattering (DLS) was 71.7 ± 0.8 nm [42], which is similar to that of the Gd-Au DENPs (89.6 ± 0.6 nm) [21]. The hydrodynamic size of the PEGylated Au DENPs-RGD was not measured in this study because the RGD modification of the NPs did not significantly change the hydrodynamic size of the Gd-Au DENP-RGD NPs and these NPs have a similar structure to the PEGylated Au DENPs-RGD (but without the additional Gd conjugation of the Gd-Au DENPs-RGD).

X-ray attenuation by the targeted PEGylated Au DENPs-RGD

We explored the possibility of using targeted PEGylated Au DENPs-RGD probes for CT imaging applications. Because Au has a higher atomic number than iodine, which is the radiodense element commonly used in conventional CT contrast agents (e.g., Omnipaque), Au NPs have been extensively utilized as contrast agents for CT imaging applications [6,8,26]. In our study, the x-ray attenuation property of the targeted PEGylated Au DENPs-RGD was compared with that of Omnipaque (Figure 4). The brightness of the CT images increases with increasing Au concentration (Figure 4A). By plotting the attenuation intensity as a function of the Au concentration, a linear response was obtained (Figure 4B). Similar to our previous reports [5,20], the attenuation intensity for both materials increases in a dose-dependent manner. However, the attenuation intensity of targeted PEGylated Au DENPs-RGD is greater than that of Omnipaque at the same Au or I concentrations, in agreement with our previous reports [21,43–44], suggesting that the PEGylated Au DENPs-RGD probes help to enhance the CT contrast, which is beneficial for targeted CT imaging applications.

Cytotoxicity assay

For biomedical applications, it is crucial to test the cytocompatibility of the targeted nanoprobes that are developed. The cytotoxicity of the PEGylated Au DENPs-RGD was assessed using an MTT assay (Figure 5). PEGylated Au DENPs-RGD display no apparent cytotoxicity at Au concentrations up to 100 μM after 24 h of incubation with either MDA-MB-435 (Figure 5A) or NK-92MI cells (Figure 5B). At the highest Au concentration tested (100 μM), both the MDA-MB-435 and NK-92MI cell viabilities are still greater than 80%, which was not significantly different from the PBS control ($p > 0.05$, $n = 3$ (Figure 5). The results here were similar to our previous study that used 200 μM Gd-Au DENPs-FA probes on KB cell (a human epithelial carcinoma cell line) [43] and 100 μM Gd-Au DENPs-RGD (Arg-Gly-Asp-Phe-Lys(mpa)) probe on U87MG cells [42]. As a result of the different properties between tumor and normal cells, our results indicate that the PEGylated Au DENP-RGD probes we developed are cytocompatible within an Au concentration range of 0–100 μM for both of these cell lines. Additionally, we further investigated the effect of PEGylated Au DENPs-RGD on the morphology of MDA-MB-435 cells by observing MDA-MB-435 cells treated with the targeted probes at different Au concentrations for 24 h (Supplementary Figure 1, see online at www.futuremedicine.com/doi/full/10.2217/NNM.15.59). The MDA-MB-435 cells treated with PEGylated Au DENPs-RGD at Au concentrations of 50–100 μM (Supplementary Figure 1B & C) display shapes that are similar to those of the cells treated with PBS (Supplementary Figure 1A).

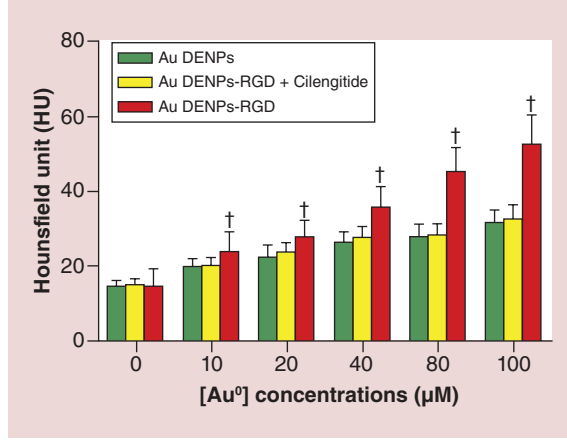

Figure 7. Computed tomography values of the cell pellets treated with nontargeted PEGylated Au DENPs, targeted nanoparticles blocked by Cilengitide and targeted PEGylated Au DENPs-RGD at different concentrations of Au for 4 h. The computed tomography values of MDA-MB-435 cells incubated with the targeted PEGylated Au DENPs-RGD were much higher than those for both the cells incubated with the nontargeted PEGylated Au DENPs and the cells treated with the targeted PEGylated Au DENPs-RGD probes but blocked by Cilengitide.
†$p < 0.01$; $n = 3$.
PEGylated Au DENPs-RGD: PEGylated dendrimer-entrapped gold nanoparticles-Arg-Gly-Asp-D-Phe-Lys.

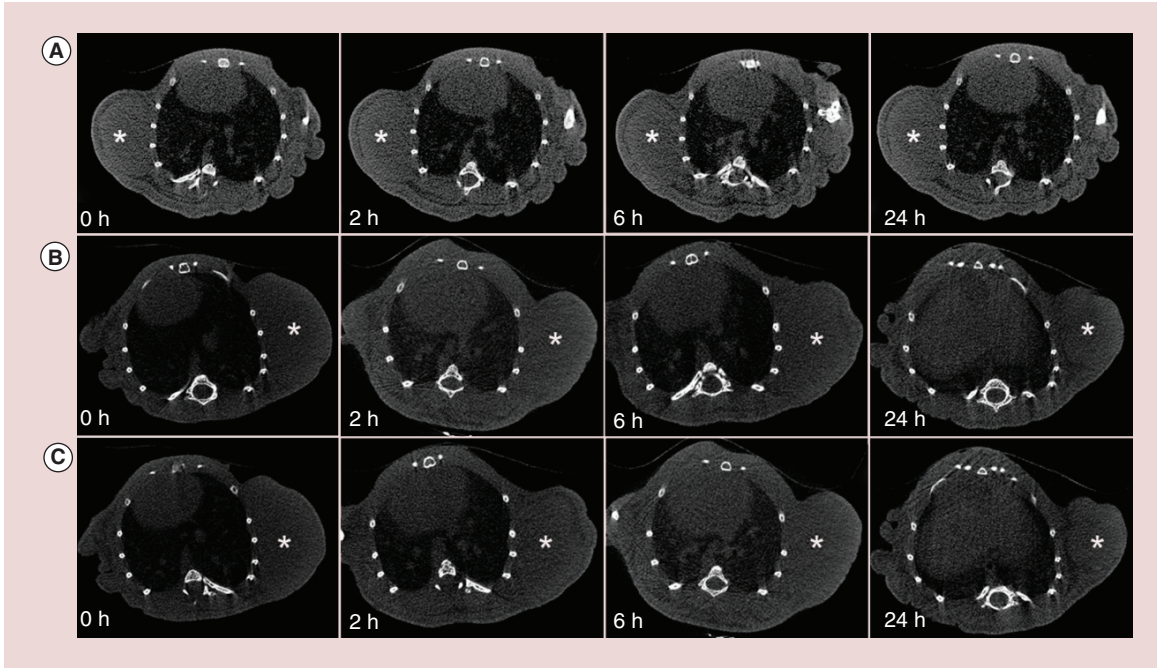

Figure 8. Representative axial CT images of mice bearing transplanted MDA-MB-435 breast cancer cells after intravenous injection of nontargeted Au DENPs (A), targeted PEGylated Au DENPs-RGD blocked by Cilengitide (B) and targeted PEGylated Au DENPs-RGD (C) for 0, 2, 6 and 24 h. The white star indicates the tumor.
CT: Computed tomography; PEGylated Au DENPs-RGD: PEGylated dendrimer-entrapped gold nanoparticles-Arg-Gly-Asp-D-Phe-Lys.

In vitro cellular uptake of PEGylated Au DENP-RGD probes

For targeted CT imaging, it is essential to investigate the ability of the PEGylated Au DENP-RGD probes to be specifically taken up by cancer cells that overexpress integrin $\alpha_v\beta_3$. ICP-AES was used to quantify Au uptake in both the MDA-MB-435 cells receiving targeted or nontargeted NPs and the MDA-MB-435 cells receiving targeted NPs but blocked with Cilengitide (a type of integrin $\alpha_v\beta_3$ inhibitor) at different Au concentrations for 4 h (Figure 6). At both Au concentrations, the Au uptake in MDA-MB-435 cells treated with targeted PEGylated Au DENPs-RGD probes is significantly higher than in cells treated with nontargeted PEGylated Au DENPs probes ($p < 0.01$, $n = 6$). Furthermore, Au uptake in MDA-MB-435 cells treated with targeted PEGylated Au DENPs-RGD probes is also much higher than in the blocked integrin $\alpha_v\beta_3$ cells that were treated with the same targeted NPs ($p < 0.01$, $n = 6$). However, Au uptake by integrin $\alpha_v\beta_3$-blocked MDA-MB-435 cells treated with targeted NPs was no different than MDA-MB-435 cells treated with nontargeted PEGylated Au DENP probes ($p > 0.05$, $n = 6$). Both of these results suggest that the PEGylated Au DENPs-RGD probes can specifically target integrin $\alpha_v\beta_3$ in overexpressed cancer cells, potentially via an integrin-mediated pathway, which is essential for these probes to be used for targeted imaging of integrin $\alpha_v\beta_3$-rich cancer cells.

In vitro targeted CT imaging of cancer cells

We next explored the possibility of using PEGylated Au DENPs-RGD probes for targeted CT imaging of cancer cells *in vitro*. MDA-MB-435cells were incubated with targeted PEGylated Au DENPs-RGD or nontargeted PEGylated Au DENPs at different Au concentrations (10, 20, 40, 80 and 100 μM) for 4 h before imaging with the clinical CT system described above. CT images were collected, and the CT values of the cells were quantified (Figure 7). Quantitative analysis of the CT images is essential because it is difficult to distinguish the brightness differences in the CT images of the cells, as described in our previous studies [4,43]. Our data clearly show that the CT values of MDA-MB-435 cells treated with both targeted PEGylated Au DENPs-RGD and nontargeted PEGylated Au DENPs are much higher than those of the corresponding cells that were treated with PBS buffer, and the CT values for both cells increase with increasing Au concentrations ($p < 0.01$, $n = 3$). At similar Au concentrations, the CT values of MDA-MB-435 cells incubated with targeted PEGylated Au DENPs-RGD are much higher than for those of the cells incubated with nontargeted PEGylated Au DENPs ($p < 0.01$, $n = 3$). However, there is no difference between the CT values of MDA-MB-435 cells treated with targeted PEGylated Au DENPs-RGD probes but blocked by Cilengitide and those treated with nontargeted PEGylated Au DENPs

at similar Au concentrations ($p > 0.05$, $n = 3$). These CT imaging findings are similar to the *in vitro* cellular uptake data and further confirm that PEGylated Au DENPs-RGD probes are targeted to cancer cells rich with integrin $\alpha_v\beta_3$.

In vivo targeted micro-CT imaging of the model tumors

To assess the targeted CT imaging of tumors, the targeted PEGylated Au DENPs-RGD or the nontargeted PEGylated Au DENPs ([Au] = 0.1 M, 200 µl) were injected intravenously via the tail vein into three groups of nude mice bearing MDA-MB-435 xenograft tumors. CT images were acquired before (0 h) and after (2, 6 and 24 h) injection using a Micro-CT system (Figure 8). Our data clearly show that the CT value at the tumor site is significantly enhanced, having a higher value after administration of both probes compared with that before the injection (Figure 9). At times postinjection, both probes could diffuse throughout the entire tumor, enabling effective tumor CT imaging. However, at each time point, the CT value for the tumor injected with the targeted PEGylated Au DENP-RGD probes is much higher than for the tumor injected with the nontargeted PEGylated Au DENPs ($p < 0.05$, $n = 8$) (Figure 9), highlighting the role that the linked RGD moieties played in specific targeting. Additionally, the CT value for the tumor injected with the targeted PEGylated Au DENPs-RGD probes is also much higher than for the tumor receiving the same targeted NPs but blocked with the integrin $\alpha_v\beta_3$ inhibitor Cilengitide ($p < 0.05$, $n = 8$) (Figure 9). This result further verifies that the PEGylated Au DENPs-RGD probes are targeted to the integrin $\alpha_v\beta_3$. The CT values for tumors treated with nontargeted PEGylated Au DENPs reached a maximum at 2 h postinjection and decreased with time postinjection. By contrast, the targeted PEGylated Au DENPs probes enhanced the tumors, even at 24 h postinjection, with 198.1% contrast enhancement, compared with the nontargeted PEGylated Au DENPs, suggesting that, due to the active RGD-mediated targeting strategy, these nanoprobes have a relatively extended retention time in the tumor tissue, enabling prolonged tumor CT imaging. Interestingly, the data demonstrate that the CT values of tumors treated with the targeted NPs but blocked by Cilengitide decreased 6 h postinjection but began to increase with time at 24 h postinjection. This likely indicates that the effectiveness of the integrin $\alpha_v\beta_3$ inhibitor Cilengitide decreased with time and that the targeted PEGylated Au DENPs-RGD probes can again associate with integrin $\alpha_v\beta_3$.

In vivo tumor uptake of PEGylated Au DENPs-RGD probes & expression of integrin $\alpha_v\beta_3$ on MDA-MB-435 xenograft tumors

To further verify that the PEGylated Au DENPs-RGD can be delivered to the tumor cells and its microenvironment for targeted CT imaging, tumor sections were stained using a silver enhancer kit and observed using a light microscope (Figure 10). In sections of tumors intravenously injected with PEGylated Au DENPs-RGD 6 h postinjection, there were numerous black spots and lines that were clearly localized in the cytoplasm of the cancer cells and the tumor endothelium, indicating the presence of the PEGylated Au DENPs-RGD (Figure 10A). There were also black spots and lines localized in the cytoplasm of cells in sections of tumors injected intravenously with nontargeted PEGylated Au DENPs and in those injected intravenously with targeted NPs but blocked with Cilengitide at 6 h postinjection but fewer than in the targeted NP-treated group. By contrast, no black spots or lines were observed in the negative control sample (Figure 10D). These results confirmed tumor uptake of the PEGylated Au DENPs-RGD via an integrin $\alpha_v\beta_3$-mediated pathway.

Immunohistochemical analysis of MDA-MB-435 xenograft tumors was performed to confirm that

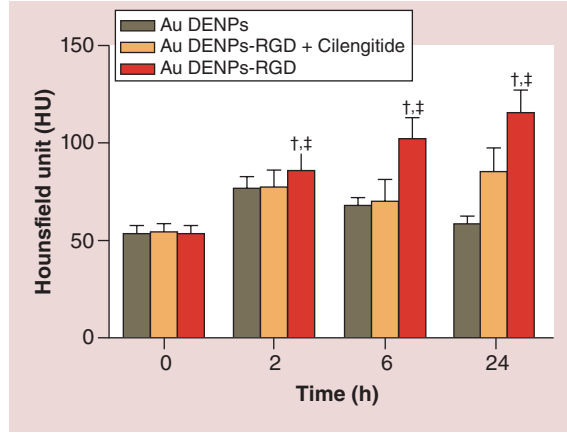

Figure 9. The CT values of mice bearing transplanted MDA-MB-435 breast cancer cells after intravenous injection of nontargeted Au DENPs, targeted PEGylated Au DENPs-RGD blocked by Cilengitide and targeted PEGylated Au DENPs-RGD for 0, 2, 6 and 24 h.
The CT value for the tumor injected with the targeted PEGylated Au DENPs-RGD probes at each time point is much higher than that for the tumor injected with the nontargeted PEGylated Au DENPs and the tumor receiving the same targeted nanoparticles but blocked with the integrin $\alpha_v\beta_3$ inhibitor Cilengitide ($p < 0.05$, $n = 8$) (Figure 9). (†$p < 0.05$ compared with nontargeted PEGylated Au DENPs, (‡$p < 0.05$ compared with targeted PEGylated Au DENPs-RGD blocked by Cilengitide.
CT: Computed tomography; PEGylated Au DENPs-RGD: PEGylated dendrimer-entrapped gold nanoparticles-Arg-Gly-Asp-D-Phe-Lys.

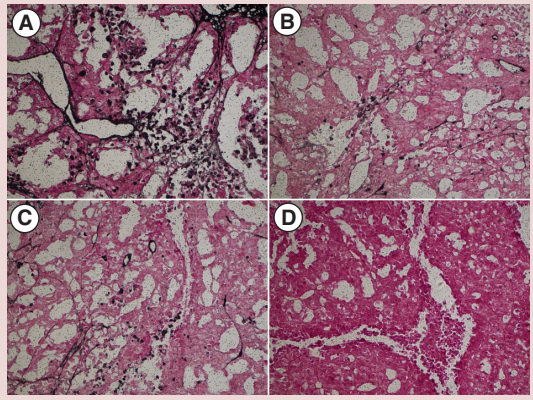

Figure 10. Silver staining optical microscope images of MDA-MB-435 xenografted mice models.
(A) Intravenous injection with targeted PEGylated Au DENPs-RGD (200 μl, [Au] = 0.1 M). **(B)** Intravenous injection with nontargeted PEGylated Gd-Au DENPs (200 μl, [Au] = 0.1 M). **(C)** Intravenous injection with targeted PEGylated Au DENPs-RGD (200 μl, [Au] = 0.1 M) blocked by Cilengitide. **(D)** Negative control without treatment. The original magnification was 200×.
PEGylated Au DENPs-RGD: PEGylated dendrimer-entrapped gold nanoparticles-Arg-Gly-Asp-D-Phe-Lys.

MDA-MB-435 xenograft tumors expressed integrin $\alpha_v\beta_3$, which enables targeted CT imaging with PEGylated Au DENPs-RGD. Supplementary Figure 2 shows the expression of integrin $\alpha_v\beta_3$ in the nude mice tumor xenograft. The brown-stained cells of the MDA-MB-435 tumor tissue are the integrin $\alpha_v\beta_3$ overexpressed cells (Supplementary Figure 2A). By contrast, there are substantially fewer brown-stained cells in the MDA-MB-435 tumor tissue blocked by Cilengitide at 2 h postintraperitoneal injection (Supplementary Figure 2B). These staining results strongly confirm the working mechanism of PEGylated Au DENPs-RGD probes for targeted CT imaging of MDA-MB-435 breast carcinoma, which is that the RGD peptides of PEGylated Au DENPs-RGD actively bind to integrin $\alpha_v\beta_3$ on MDA-MB-435 breast cancer; then, the nanoprobes are phagocytosed by the targeted cells, enabling effective targeted CT imaging of the MDA-MB-435 xenograft tumors. Several previous studies have investigated the antibody-targeted NPs on breast cancer, yet the large size, difficulty in conjugation to NPs and other limitations hamper its broad application [45,46]. In comparison to antibody-targeted NPs, the RGD-targeted NPs have several advantages, including small size, low immunogenicity and relatively low cost [46]. Therefore, we anticipate that this RGD-targeted NP might have better prospects than antibody-targeted NPs.

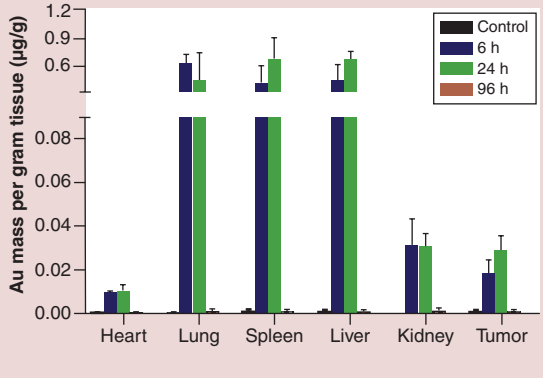

Figure 11. Biodistribution of Au in the major organs of the mice, including the heart, liver, spleen, lung, kidney and tumor. The data were recorded for the entire organ at different time points postintravenous injection of PEGylated Au DENPs-RGD probes (200 μl, [Au] = 0.1 M).
PEGylated Au DENPs-RGD: PEGylated dendrimer-entrapped gold nanoparticles-Arg-Gly-Asp-D-Phe-Lys.

In vivo biodistribution of PEGylated Au DENPs-RGD probes

The biodistribution (Au uptake) of the targeted NPs in the major organs, including the heart, lungs, spleen, liver, kidneys and tumors, was analyzed using ICP-AES (Figure 11). The data show that the liver and spleen have significant Au accumulation at 6 and 24 h postinjection with Au levels of 446 μg/g (6 h) and 564 μg/g (24 h) in the liver and 415 μg/g (6 h) and 681 μg/g (24 h) in the spleen. The PEGylation of the NPs appears to allow a portion of the particles to escape recognition by the reticuloendothelial system in the liver and spleen with accumulation in tumors and other organs, such as the heart, lungs and kidneys [47,48]. Due to the RGD-mediated active targeting and the benefit of a prolonged circulation time because of PEGylation modification [21], the PEGylated Au DENPs-RGD probes can gradually accumulate in the tumors, with an Au uptake of 18.5 μg/g (6 h) and 28.8 μg/g (24 h), enabling effective CT-targeted imaging, similar to our previous Gd-Au DENP-FA probes [43] and Gd-Au DENP-RGD probes [42]. However, at 96 h postinjection, the Au uptake in all of the major organs almost approached the same level before injection, which suggested that the NPs can be eliminated from the body, which is very important for clinical biomedical imaging applications.

Conclusion

In summary, we developed a PEGylated dendrimer-based integrin $\alpha_v\beta_3$-targeted nanoprobe for CT imaging of tumors. Because of multifunctional dendrimer nanotechnology, Au NPs can be entrapped within the

dendrimer and modified on the dendrimer surface. As a result of the PEGylation modification and the integrin $\alpha_v\beta_3$-mediated targeting pathway, the functional nanoprobes developed here are effective for targeted CT imaging of cancer cells and tumor xenografts that overexpress integrin $\alpha_v\beta_3$ *in vitro* and *in vivo*. The nanoprobes are stable colloids, water soluble and have good cytocompatibility in the given concentration range. *In vitro* cellular and *in vivo* tumor uptake studies of PEGylated Au DENPs-RGD probes and expression of integrin $\alpha_v\beta_3$ on MDA-MB-435 xenograft tumors confirm that the designed NPs target cancer cells. In addition, biodistribution studies show that the targeted nanoprobes can be eliminated from the body 96 h after injection. The unique structural characteristics of the dendrimers allow them to be linked with different ligands or drugs, and functional nanoprobes with other targeting functionalities can most likely be developed for targeted CT imaging of different types of tumors.

Future perspective

An increasing number of studies report the application of RGD peptide-targeted tumors for cancer diagnosis and therapy. The designed PEGylated Au DENPs-RGD can be used as a targeted nanoprobe with good biocompatibility for targeted CT imaging and diagnosis of integrin-positive tumors. This functional nanoprobe can most likely be developed for the targeted CT imaging of different types of tumors. A large animal model and translational study are urgently needed.

Financial & competing interests disclosure

This research is financially supported by the National Natural Science Foundation of China (21273032, 81101150, 81271384, 81201132 and 81371623), the Shanghai Pujiang Project (KAL 2014PJD028), the State Scholarship Fund by China Scholarship Council for Linfeng Zheng and 'The Best Youth Medical Scholars' fund by Shanghai First People's Hospital, Shanghai Jiao Tong University for L Zheng, the Shanghai Natural Science Foundation (11ZR1429300 and 12ZR1424900), the Medical Guiding Program of Shanghai Science and Technology Committee (114119a0800). The authors have no other relevant affiliations or financial involvement with any organization or entity with a financial interest in or financial conflict with the subject matter or materials discussed in the manuscript apart from those disclosed.

No writing assistance was utilized in the production of this manuscript.

Ethical conduct of research

The authors state that they have obtained appropriate institutional review board approval or have followed the principles outlined in the Declaration of Helsinki for all human or animal experimental investigations. In addition, for investigations involving human subjects, informed consent has been obtained from the participants involved.

Executive summary

- We report the synthesis and characterization of cyclo (Arg-Gly-Asp-D-Phe-Lys) peptide (RGD)-modified PEGylated dendrimer-entrapped gold nanoparticles (Au DENPs) and demonstrate that PEGylated Au DENPs-RGD with an Au nanoparticle (NP) core size of 2.8 nm are water dispersible, stable at different pH and temperature conditions, and biocompatible over the given concentration range. In the presence of Au NPs, the PEGylated Au DENPs-RGD displayed high x-ray attenuation intensities. The conjugated RGD ligand can specifically identify and target overexpressed integrins on cancer cells. Moreover, the accumulation of the NPs in the target area allows them to be used as nanoprobes for targeted computed tomography imaging of integrin-rich breast carcinoma cells *in vitro* and xenograft tumor models *in vivo*.

References

Papers of special note have been highlighted as:
• of interest; •• of considerable interest

1 Kobayashi H, Longmire MR, Ogawa M, Choyke PL, Kawamoto S. Multiplexed imaging in cancer diagnosis: applications and future advances. *Lancet Oncol.* 11(6), 589–595 (2010).

2 Reuveni T, Motiei M, Romman Z, Popovtzer A, Popovtzer R. Targeted gold nanoparticles enable molecular CT imaging of cancer: an *in vivo* study. *Int. J. Nanomedicine* 6, 2859–2864 (2011).

•• ***In vivo* study on antiepidermal growth factor receptor-targeted gold nanoparticles for tumour computed tomography (CT) imaging.**

3 Rabin O, Perez JM, Grimm J, Wojtkiewicz G, Weissleder R. An x-ray computed tomography imaging agent based on long-circulating bismuth sulphide nanoparticles. *Nat. Mater.* 5(2), 118–122 (2006).

4 Peng C, Li K, Cao X *et al.* Facile formation of dendrimer-stabilized gold nanoparticles modified with diatrizoic acid for enhanced computed tomography imaging applications. *Nanoscale* 4, 6768–6778 (2012).

5 Peng C, Zheng L, Chen Q *et al.* PEGylated dendrimer-entrapped gold nanoparticles for *in vivo* blood pool and tumor imaging by computed tomography. *Biomaterials* 33(4), 1107–1119 (2012).

•• **PEGylated dendrimer-entrapped gold nanoparticles (Au DENPs) can be used as a promising contrast agent.**

6 Popovtzer R, Agrawal A, Kotov NA *et al.* Targeted gold nanoparticles enable molecular CT imaging of cancer. *Nano Lett.* 8(12), 4593–4596 (2008).

7 Yordanov AT, Lodder AL, Woller EK *et al.* Novel iodinated dendritic nanoparticles for computed tomography (CT) imaging. *Nano Lett.* 2(6), 595–599 (2002).

8 Kim D, Park S, Lee JH, Jeong YY, Jon S. Antibiofouling polymer-coated gold nanoparticles as a contrast agent for *in vivo* x-ray computed tomography imaging. *J. Am. Chem. Soc.* 129(24), 7661–7665 (2007).

•• **PEG-coated gold nanoparticles can be useful as a CT contrast agent for blood pool and hepatoma imaging.**

9 Kim SH, Kamaya A, Willmann JK. CT perfusion of the liver: principles and applications in oncology. *Radiology* 272(2), 322–344 (2014).

10 Taherian A, Li X, Liu Y, Haas TA. Differences in integrin expression and signaling within human breast cancer cells. *BMC Cancer* 11, 293 (2011).

11 Zhou Y, Chakraborty S, Liu S. Radiolabeled cyclic RGD peptides as radiotracers for imaging tumors and thrombosis by SPECT. *Theranostics* 1, 58–82 (2011).

12 Danhier F, Le Breton A, Preat V. RGD-based strategies to target alpha($_v$) beta($_3$) integrin in cancer therapy and diagnosis. *Mol. Pharm.* 9(11), 2961–2973 (2012).

13 Liu Z, Wang F, Chen X. Integrin alpha($_v$)beta($_3$)-targeted cancer therapy. *Drug Dev. Res.* 69(6), 329–339 (2008).

14 Desgrosellier JS, Cheresh DA. Integrins in cancer: biological implications and therapeutic opportunities. *Nat. Rev. Cancer* 10(1), 9–22 (2010).

15 Zitzmann S, Ehemann V, Schwab M. Arginine-glycine-aspartic acid (RGD)-peptide binds to both tumor and tumor-endothelial cells *in vivo*. *Cancer Res.* 62(18), 5139–5143 (2002).

•• **Arginine-glycine-aspartic acid (RGD) peptide can target tumour endothelial cells as well as tumour cells.**

16 Wang H, Zheng L, Peng C, Shen M, Shi X, Zhang G. Folic acid-modified dendrimer-entrapped gold nanoparticles as nanoprobes for targeted CT imaging of human lung adencarcinoma. *Biomaterials* 34, 470–480 (2013).

• **Folic acid-targeted Au DENPs can be used as imaging probes for targeted CT imaging.**

17 Dixit S, Novak T, Miller K, Zhu Y, Kenney ME, Broome AM. Transferrin receptor-targeted theranostic gold nanoparticles for photosensitizer delivery in brain tumors. *Nanoscale* 7(5), 1782–1790 (2014).

18 Jiang X, Sha X, Xin H *et al.* Self-aggregated pegylated poly (trimethylene carbonate) nanoparticles decorated with c(RGDyK) peptide for targeted paclitaxel delivery to integrin-rich tumors. *Biomaterials* 32(35), 9457–9469 (2011).

19 Fede C, Fortunati I, Weber V *et al.* Evaluation of gold nanoparticles toxicity towards human endothelial cells under static and flow conditions. *Microvasc. Res.* 97, 147–155 (2015).

20 Wang H, Zheng L, Peng C *et al.* Computed tomography imaging of cancer cells using acetylated dendrimer-entrapped gold nanoparticles. *Biomaterials* 32(11), 2979–2988 (2011).

21 Wen S, Li K, Cai H *et al.* Multifunctional dendrimer-entrapped gold nanoparticles for dual mode CT/MR imaging applications. *Biomaterials* 34(5), 1570–1580 (2013).

•• **Gd-Au DENPs as a dual mode contrast agent.**

22 Delong RK, Reynolds CM, Malcolm Y, Schaeffer A, Severs T, Wanekaya A. Functionalized gold nanoparticles for the binding, stabilization, and delivery of therapeutic DNA, RNA, and other biological macromolecules. *Nanotechnol. Sci. Appl.* 3, 53–63 (2010).

23 Dreaden EC, Austin LA, Mackey MA, El-Sayed MA. Size matters: gold nanoparticles in targeted cancer drug delivery. *Ther. Deliv.* 3(4), 457–478 (2012).

24 Tomalia DA, Frechet JMJ. *Dendrimers And Other Dendritic Polymers.* John Wiley & Sons Ltd, NY, USA (2001).

25 Guo R, Wang H, Peng C *et al.* Enhanced x-ray attenuation property of dendrimer-entrapped gold nanoparticles complexed with diatrizoic acid. *J. Mater. Chem.* 18(13), 5120–5127 (2011).

26 Guo R, Wang H, Peng C *et al.* X-ray attenuation property of dendrimer-entrapped gold nanoparticles. *J. Phys. Chem. C* 114(1), 50–56 (2010).

• **Au DENPs can be used as a CT contrast agent.**

27 Liu H, Shen M, Zhao J *et al.* Tunable synthesis and acetylation of dendrimer-entrapped or dendrimer-stabilized gold–silver alloy nanoparticles. *Colloid Surf. B Biointerfaces* 94, 58–67 (2012).

28 Liu H, Wang H, Guo R *et al.* Size-controlled synthesis of dendrimer-stabilized silver nanoparticles for x-ray computed tomography imaging applications. *Polym. Chem.* 1(10), 1677–1683 (2010).

29 Liu H, Xu Y, Wen S *et al.* Facile hydrothermal synthesis of low generation dendrimer-stabilized gold nanoparticles for *in vivo* computed tomography imaging applications. *Polym. Chem.* 4, 1788–1795 (2013).

30 Peng C, Wang H, Guo R *et al.* Acetylation of dendrimer-entrapped gold nanoparticles: synthesis, stability, and x-ray attenuation properties. *J. Appl. Polym. Sci.* 119(3), 1673–1682 (2011).

31 Shen M, Shi X. Dendrimer-based organic/inorganic hybrid nanoparticles in biomedical applications. *Nanoscale* 2(9), 1596–1610 (2010).

32 Kukowska-Latallo JF, Candido KA, Cao Z *et al.* Nanoparticle targeting of anticancer drug improves therapeutic response in animal model of human epithelial cancer. *Cancer Res.* 65(12), 5317–5324 (2005).

33 Majoros IJ, Myc A, Thomas T, Mehta CB, Baker JR. PAMAM dendrimer-based multifunctional conjugate for cancer therapy: synthesis, characterization, and functionality. *Biomacromolecules* 7(2), 572–579 (2006).

• **The synthesis, characterization and functionality strategy of different dendrimer conjugates for cancer therapy.**

34 Thomas TP, Majoros IJ, Kotlyar A *et al.* Targeting and inhibition of cell growth by an engineered dendritic nanodevice. *J. Med. Chem.* 48, 3729–3735 (2005).

35 Nwe K, Bryant LH Jr, Brechbiel MW. Poly (amidoamine) dendrimer based MRI contrast agents exhibiting enhanced

relaxivities derived via metal preligation techniques. *Bioconjug. Chem.* 21(6), 1014–1017 (2010).

36 Shi X, Thomas TP, Myc LA, Kotlyar A, Baker JR Jr. Synthesis, characterization, and intracellular uptake of carboxyl-terminated poly(amidoamine) dendrimer-stabilized iron oxide nanoparticles. *Phys. Chem. Chem. Phys.* 9(42), 5712–5720 (2007).

37 Shi X, Lee I, Baker JR Jr. Acetylation of dendrimer-entrapped gold and silver nanoparticles. *J. Mater. Chem.* 18(5), 586–593 (2008).

38 Majoros IJ, Keszler B, Woehler S, Bull T, Baker JR Jr. Acetylation of poly(amidoamine) dendrimers. *Macromolecules* 36(15), 5526–5529 (2003).

39 Rasband WS. ImageJ, NIH. http://rsb.info.nih.gov/ij/download.html

40 Burke PA, Denardo SJ, Miers LA, Lamborn KR, Matzku S, Denardo GL. Cilengitide targeting of alpha($_v$)beta($_3$) integrin receptor synergizes with radioimmunotherapy to increase efficacy and apoptosis in breast cancer xenografts. *Cancer Res.* 62(15), 4263–4272 (2002).

41 Shi X, Wang S, Meshinchi S *et al.* Dendrimer-entrapped gold nanoparticles as a platform for cancer-cell targeting and imaging. *Small* 3(7), 1245–1252 (2007).

42 Chen Q, Wang H, Liu H *et al.* Multifunctional dendrimer-entrapped gold nanoparticles modified with RGD peptide for targeted CT/MR dual modal imaging of tumors. *Anal. Chem.* 87(7), 3949–3956 (2015).

43 Chen Q, Li K, Wen S *et al.* Targeted CT/MR dual mode imaging of tumors using multifunctional dendrimer-entrapped gold nanoparticles. *Biomaterials* 34(21), 5200–5209 (2013).

44 Li K, Wen S, Larson AC *et al.* Multifunctional dendrimer-based nanoparticles for *in vivo* MR/CT dual-modal molecular imaging of breast cancer. *Int. J. Nanomedicine* 8, 2589–2600 (2013).

45 Sun B, Ranganathan B, Feng SS. Multifunctional poly(D,L-lactide-co-glycolide)/montmorillonite (PLGA/MMT) nanoparticles decorated by Trastuzumab for targeted chemotherapy of breast cancer. *Biomaterials* 29(4), 475–486 (2008).

• **A therapeutical nanoparticle for targeted chemotherapy of breast cancer.**

46 Yu MK, Park J, Jon S. Targeting strategies for multifunctional nanoparticles in cancer imaging and therapy. *Theranostics* 2(1), 3–44 (2012).

47 Moghimi SM, Hunter AC, Murray JC. Nanomedicine: current status and future prospects. *FASEB J.* 19(3), 311–330 (2005).

48 Liu Z, Cai W, He L *et al. In vivo* biodistribution and highly efficient tumour targeting of carbon nanotubes in mice. *Nat. Nanotechnol.* 2(1), 47–52 (2007).